Ultrathin Optical Fibers : Guided Modes, Angular Momentum, and Applications

Laser Review

Ultrathin Optical Fibers: Guided Modes, Angular Momentum, and Applications

Cindy Liza ESPORLAS,[1] Georgiy TKACHENKO,[1] Viet Giang TRUONG,[1] and Síle NIC CHORMAIC[1,2]

[1]*Light-Matter Interactions Unit, Okinawa Institute of Science and Technology Graduate University, Onna, Okinawa 904-0495, Japan*

[2]*Laboratoire Aimé Cotton, CNRS, Université Paris-Sud, ENS Cachan, Université Paris-Saclay, 91405 Orsay Cedex, France*

(Received November 30, 2017)

Ultrathin optical fibers have emerged as efficient and versatile platforms for studying light-matter interactions. Owing to their geometry, they are characterized by intense evanescent fields extending beyond the fiber surface. These fields can carry both spin and orbital angular momentum of guided light. Complex spatial intensity, phase, and polarization profiles can be generated at the fiber waist by propagating higher order fiber modes. In this paper, we review applications of ultrathin optical fibers, with an emphasis on optical manipulation at the micro- and nanoscale. We also discuss mode content and angular momentum of light guided by ultrathin fibers.

Key Words: Ultrathin Fiber, Higher Order Mode, Angular Momentum, Evanescent Field, Particle Manipulations

1. Introduction

The phenomenon of light's angular momentum is the core of an actively developing field which covers both fundamental and application-oriented studies in optics. In paraxial optics, where the transverse dimensions of a light beam are much smaller than typical longitudinal ones, the total angular momentum of light is a superposition of two distinct components, i.e. spin and orbital.[1)] Spin angular momentum (SAM) is related to circular polarization, as experimentally demonstrated by Beth in 1936.[2)] In contrast, orbital angular momentum (OAM) does not depend on polarization, but is an explicit function of the spatial coordinates. Separation of the spin and orbital parts of angular momentum has been experimentally verified by observing light-induced rotational motion of dielectric microparticles trapped in a circularly polarized vortex beam.[3)] Harnessing SAM and OAM of light has led to the development of novel techniques for optical manipulation,[4)] life sciences,[5)] astronomy,[6,7)] telecommunications,[8)] atomic[9)] and quantum physics.[10)]

Besides free-space methods, optical angular momentum can be delivered to a system via an optical fiber, which is a key element in modern telecommunications, and various devices for generation, amplification, shaping, detection, and analysis of light. The rise in demand for highly precise and stable control and manipulation of small particles for different applications has led to the use of light field modifying structures, such as ultrathin optical fibers (UOFs).[11,12)] Such fibers, with diameters comparable or smaller than the wavelength of light, can be readily fabricated by tapering conventional silica fibers via controlled heating and pulling.[13)] An UOF can collect and deliver light through the evanescent fields at its waist, thereby allowing longer interaction distances compared to what could be achieved using tightly focused free-space beams which are limited by the Rayleigh range. UOFs represent a versatile and powerful platform for studying light-matter interactions from both classical and quantum points of view.[14,15)] Because of the tight confinement of light at the fiber waist, the paraxial approximation is not valid. This leads to spin-orbit angular momentum coupling, which is expected to have an effect on light-induced motion of particles near the fiber surface. For example, besides the naturally expected SAM, a quasi-circularly polarized fundamental mode (FM) of an UOF also carries OAM whose density strongly depends on the fiber waist diameter.[16)]

UOFs show great potential for advancing atomic and quantum physics. Recently, OAM storage[17,18)] and the enhancement of multipole transitions in atoms interacting with higher order modes (HOMs) of an UOF[19)] have been proposed. In this brief review, we discuss the properties and applications of UOF guided light. Special attention is paid to HOMs and angular momentum.

2. Ultrathin Optical Fibers

Figure 1 represents a typical UOF fabricated from a single-mode, step-index glass fiber. Low loss transmission of the target set of modes is provided by adiabatic tapering and surface smoothness of the fiber. Tapering is typically performed by means of oxy-hydrogen flame brushing and controlled pulling according to a pre-calculated geometrical profile while monitoring transmission of either the FM or HOMs.[23)] The fi-

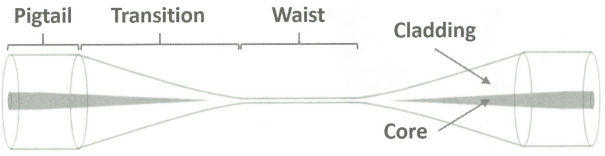

Fig. 1 Schematic of an UOF structure, which includes unmodified pigtails on both ends, a smooth transition region providing adiabatic guiding, and a waist region of a constant radius and custom designed length.

ber structure consists of the ultrathin waist linked to the unmodified pigtails via transition regions typically being an exponential, linear or poly-linear function of the radius versus the longitudinal coordinate. Along with the cladding refractive index, the waist radius is the key geometrical parameter of an UOF. In the pigtail, light is weakly guided in the form of linearly polarized (LP) modes. Moving into the transition region, the modes become cladding guided with a growing evanescent field amplitude. The mode content of a particular UOF is determined by a characteristic waveguide size parameter, $V = 2\pi aNA / \lambda$, where a is the final waist radius, NA is the fiber numerical aperture, and λ is the free-space wavelength of the guided light. As the fiber thins, the propagation constant β gradually reduces and higher-order LP mode groups eventually cease to propagate, as shown in Fig. 2.[20,21] The most commonly applied in UOFs are the fundamental mode (LP_{01}: $HE_{11o,e}$) and the first group of HOMs (LP_{11}: TE_{01}, TM_{01}, $HE_{21o,e}$), see the insets in Fig. 2. A theoretical and experimental demonstration of the first six modes in UOFs have been reported by Petcu-Colan *et al.*[22] and Frawley *et al.*[23]

Mode coupling in an UOF is dependent both on the input field and fiber geometry. Therefore, in practice, it is not possible to predict the mode content at the UOF waist in a particular experimental situation. However, the modes can be detected by Rayleigh scattering imaging from the fiber surface.

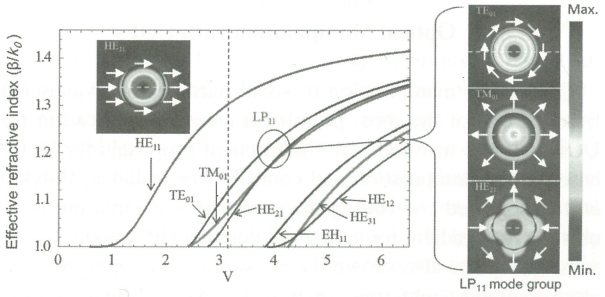

Fig. 2 Simulated geometrical dependence of the propagation constants of various modes supported by a vacuum-clad UOF. The insets show the intensity (false colors) and polarization (arrows) profiles for the FM and the LP_{11} group. Reproduced from.[24]

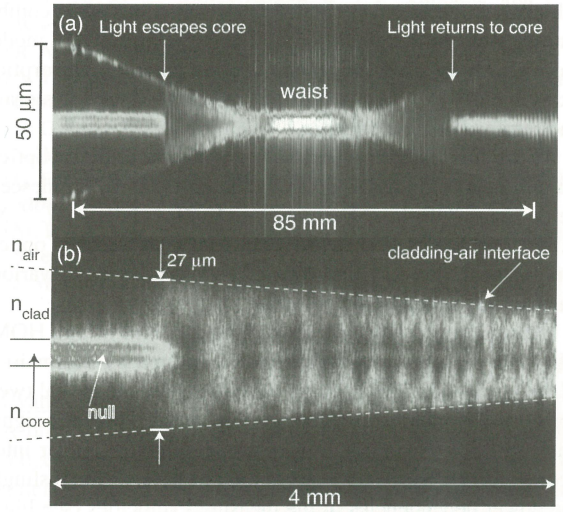

Fig. 3 Direct imaging of Rayleigh scattered light allows visualization of mode pair beatings in an UOF. Here λ = 795 nm and the fiber waist radius equals 1.5 µm. Reproduced from.[27]

This method has been introduced by Eickhoff and Krumpholz for conventional single-mode fibers in 1976.[25] It has been further developed in the recent studies by Fatemi *et al.*[26] and Hoffman *et al.*[27] who demonstrated precise detection and even control of the mode content at the waist of a few-mode UOF.

Apart from direct imaging, Fatemi *et al.*[28] detected scattered light with even higher precision by means of scanning with a single-mode fiber probe in order to read the intensity changes along the UOF under study, see Fig. 4(inset). This non-invasive technique gives information about the mode content based on spatial beating frequencies of different mode combinations, as presented by the diagram in Fig. 4. Moreover, the modal interference allows one to estimate the local UOF radius *in situ* with the extraordinary precision of 0.01 nm.[28] Potentially, this technique of scattering field analysis can be combined with the modal transfer matrix measurement method developed for multimode fibers by Carpenter *et al.*[29] This seems to be a promising way towards the 'holy grail' for applications involving HOMs in UOFs, namely a reliable method to control the modes at the ultrathin waist by addressing only the input and output fields at the pigtails. The need for such a method is getting more critical with the growing interest in angular momentum of light delivered by UOFs via HOMs.

3. Angular momentum in UOF

The angular momentum of light in fibers is usually described using the generally accepted Abraham formulation where the field-only contribution to light's momentum inside and outside of the fiber is considered. For the FM propagating through a vacuum-clad UOF, the changing fiber radius, core-cladding refractive index difference, and polarization significantly influence the evanescent field distribution near the fiber surface.[20] Studies by Le Kien *et al.* determined the spin and orbital components of the finite total angular momentum of a quasi-circularly polarized HE_{11} mode in a vacuum-clad silica UOF.[16] The Poynting vector in the evanescent field of this mode follows a helical trajectory around the UOF waist, as sketched in Fig. 5. By using the axial and azimuthal Poynting vector components, SAM and OAM densities around the waist have been calculated. It has been found that for $a \ll \lambda$, the total angular momentum contains only SAM which in fact dominates at any radius a. Interestingly, sub-

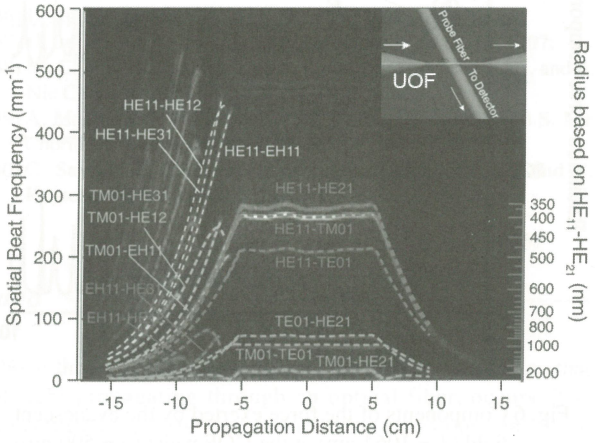

Fig. 4 *In situ* mode detection and analysis by means of a coupled single-mode probe fiber (inset). The right ordinate shows the corresponding fiber radius estimation. Reproduced from.[28]

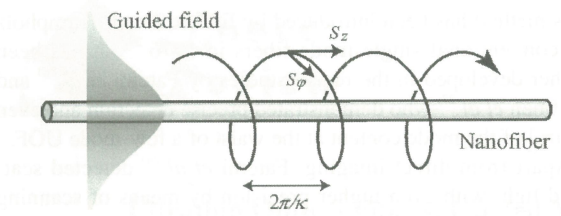

Fig. 5 Helical trajectory of the Poynting vector in the evanescent field of a quasi-circularly polarized FM of an UOF. Reproduced from.[16]

stantial OAM appears for intermediate waist radii ($a \approx \lambda$). As the fiber gets thicker ($a \gg \lambda$), the OAM density vanishes giving a limiting value for the total and spin angular momenta.

A spherical dielectric particle placed near the surface of an UOF waist experiences scattering, F_z, and gradient, F_r, forces exerted by the guided evanescent field. A peculiar result predicted for the quasi-circularly polarized FM is the negative azimuthal force, F_ϕ, (see Fig. 6(b)) exerted on a dielectric particle interacting with the evanescent field at the UOF waist. This negative azimuthal force arises from the momentum transfer to particles when quasi-circularly polarized light is scattered dominantly in the same direction as the azimuthal Poynting vector component.[30]

In the case of HOMs, Le Kien *et al.* have found interesting behavior of hybrid HE and EH modes in vacuum-clad UOFs. Figure 7 presents the angular momentum per photon as a function of fiber radius, a, for quasi-circularly polarized hybrid modes. The orbital component increases with higher azimuthal mode index and can become more dominant than the spin component.[21] Additionally, it has been also predicted that EH modes must have a negative axial component for the spin and surface angular momenta with respect to the phase circulation direction. The negative azimuthal component of the Poynting vector and the spin angular momentum with respect to the phase circulation direction can result in novel effects that are yet to be studied through optomechanical experiments by observation of light-induced rotation of micro- or nanoparticles around the UOF waist. As a further development, one may employ anisotropic particles in order to distinguish the spin and orbital components of the mechanical angular momentum transfer.

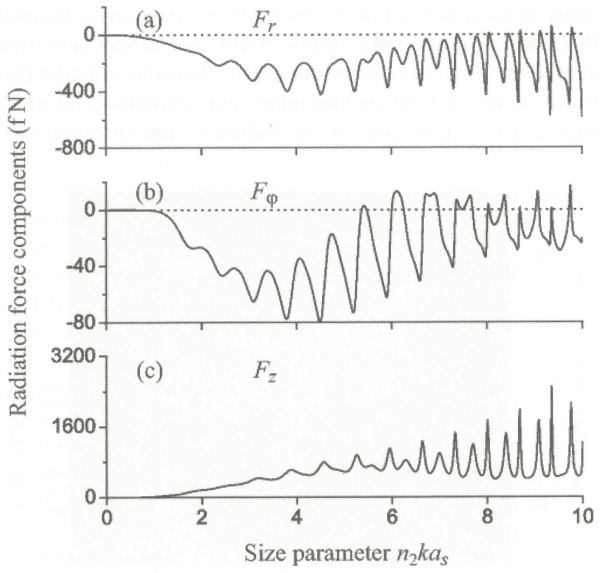

Fig. 6 Components of the force exerted by the evanescent field (λ = 1064 nm) at the UOF waist (a = 500 nm) on a dielectric microsphere placed near the fiber surface in water (n_2 = 1.33). Oscillations arise from Mie resonances associated with whispering gallery modes in the microsphere. Reproduced from.[30]

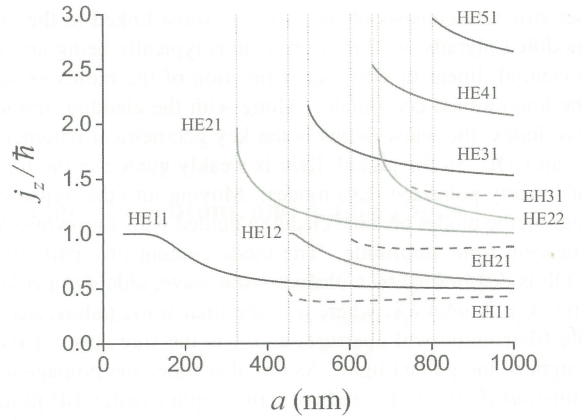

Fig. 7 Calculated angular momentum per photon as a function of the fiber radius, a, for quasi-circularly polarized UOF hybrid modes with positive phase circulation direction. Vertical dotted lines indicate the cutoff positions. Reproduced from.[21]

4. Optical Manipulation with UOFs

Contactless manipulation of small particles by evanescent fields is one of the most prominent areas of application for UOFs. It has inspired many theoretical proposals for UOF-based atom manipulation and control. For instance, Balykin *et al.* suggested controlling the center-of-mass motion of atoms via the gradient force of a red-detuned HE_{11} mode.[19] The same group has also shown the possibility of creating various atom trapping geometries, such as two parallel lines or a cylindrical shell, by using a two-color HE_{11} evanescent field with either linear or circular polarization.[33] Using a similar two-color scheme, but employing interference between co-propagating blue-detuned FM and a red-detuned HOM, a flexible 1D trapping lattice for Cs atoms has been proposed by Fu *et al.*[34] More complex interference patterns, such as a 4-helix configuration, generated from two-color HOM combinations were further explored by Phelan *et al.*[32] UOF modes have also been used for atomic fluorescence and absorption experiments[24,40] where UOFs act as an interface for storage and retrieval of light pulses.

At the microscale, experimental demonstration of optical trapping and propulsion of dielectric particles by evanescent fields from UOFs have been realized by Brambilla *et al.*[35] Xu *et al.*[36] and Lei *et al.*[37] have reported on UOF-assisted optical arrangement, delivery, and size-dependent trapping of various particles including living bacteria.

Interactions of dielectric microspheres with FM and HOMs of UOFs have been experimentally explored by Maimaiti *et al.* by means of a UOF system combined with an optical tweezer setup.[31,39] The micrographs in Fig. 8(left) show the significant (8-fold) enhancement of particle velocities under interaction with HOMs as opposed to the FM case.[31] Interestingly, the power dependencies of the measured velocities (see Fig 8, right) show nonlinear behavior for HOMs. This effect suggests yet unexplored complex hydrodynamic interactions between the guided particle and the fiber. Further studies with multiple trapped particles at the UOF surface have revealed

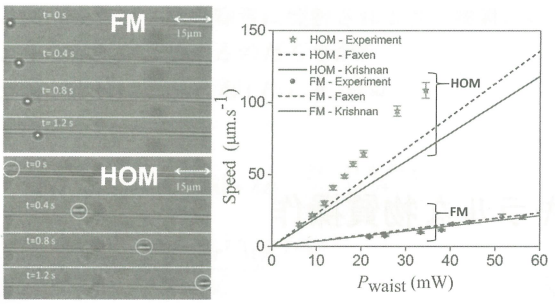

Fig. 8 Left: Successive microscope images demonstrating light-induced propulsion of a 3 μm polystyrene microsphere under FM and HOM propagation with the optical power 25 mW in both cases. The enhanced light-matter interaction for the HOM leads to 8-fold faster propulsion. Right: Measured particle speed versus optical power reveals the nonlinear behavior attributed to yet unexplored hydrodynamic effects. Reproduced from Ref. 31).

1D longitudinal self-arrangement through optical binding.[38,39] Future prospects for optical manipulation with UOFs mainly involve the spinning and rotational motion of dielectric particles due to spin and orbital angular momentum transfer.

5. Conclusion

In this paper we have reviewed applications of UOFs for manipulation and control of various material objects ranging from atoms to micro-scale dielectric particles. Despite many theoretical studies on light-matter interactions mediated by evanescent fields around UOFs, practical realizations are surprisingly scarce. We attribute this fact to the experimental challenges arising when HOMs are involved. Indeed, reliable control of mode content at the ultrathin fiber waist appears to be a hard technical challenge which has to be tackled. We envisage further experimental work dedicated to understanding the physics of angular momentum carried by evanescent fields of UOFs.

References

1) L. Allen, M. W. Beijersbergen, R. J. C. Spreeuw, and J. P. Woerdman: Phys. Rev. A **45** (1992) 8185.
2) R. A. Beth: Physical Review **50** (1936) 115.
3) A. T. O'Neil, I. MacVicar, L. Allen, and M. J. Padgett: Phys. Rev. Lett. **88** (2002) 053601.
4) D. G. Grier: Nature **424** (2003) 810.
5) S. W. Hell and J. Wichmann: Opt. Lett. **19** (1994) 780.
6) G. Foo, D. M. Palacios, and G. Swartzlander: Opt. Lett. **30** (2005) 3308.
7) M. P. J. Lavery, F. C. Speirits, S. M. Barnett, and M. J. Padgett: Science **341** (2013) 537.
8) J. Wang, J. Yang, I. M. Fazal, N. Ahmed, Y. Han, H. Huang, Y. Ren, Y. Yue, S. Dolinar, M. Tur, *et al.*: Nature Photonics **6** (2012) 488.
9) S. Franke-Arnold: Philo. Trans. of the Royal Soc. London A: Mathematical, Physical and Engineering Sciences **375** (2017) 2087.
10) Z. Zhou, Y. Li, D. Ding, W. Zhang, S. Shi, B. Shi, and G. Guo: Light: Sci. & Applns. **5** (2016) e16019.
11) M. Daly, V. G. Truong, and S. Nic Chormaic: Opt. Express **24** (2016) 14470.
12) M. Sergides, V. G. Truong, and S. Nic Chormaic: Nanotechnology **27** (2016) 365301.
13) J. M. Ward, A. Maimaiti, V. H. Le, and S. Nic Chormaic: Rev. Sci. Instru. **85** (2014) 111501.
14) X. Wu and L. Tong: Nanophot. **2** (2013) 407.
15) P. Solano, J. A. Grover, J. E. Hoffman, S. Ravets, F. K. Fatemi, L. A. Orozco, and S. L. Rolston: Adv. A. M. O. P. **66** (2017) 439.
16) F. Le Kien, V. I. Balykin, and K. Hakuta: Phys. Rev. A **73** (2006) 053823.
17) A. Nicolas, L. Veisser, L. Giner, E. Giacobino, D. Mazxein, and J. Laurat: Nat. Phot. **8** (2014) 234.
18) D. Ding, W. Zhang, Z. Zhou, S. Shi, G. Xiang, X. Wang, Y. Jiang, B. Shi, and G. Guo: Phys. Rev. Lett. **114** (2015) 020502.
19) V. I. Balykin, K. Hakuta, F. Le Kien, J. Q. Liang, and M. Morinaga: Phys. Rev. A **70** (2004) 011401.
20) F. Le Kien, J. Q. Liang, K. Hakuta, and V. I. Balykin: Opt. Commun. **242** (2004) 445.
21) F. Le Kien, T. Busch, V. G. Truong, and S. Nic Chormaic: Phys. Rev. A **96** (2017) 023835.
22) A. Petcu-Colan, M. Frawley, and S. Nic Chormaic: J. of Nonlin. Opt. Phys. and Mat. **20** (2011) 293.
23) M. C. Frawley, A. Petcu-Colan, V. G. Truong, and S. Nic Chormaic: Opt. Commun. **285** (2012) 4648.
24) R. Kumar, V. Gokhroo, K. Deasy, A. Maimaiti, M. C. Frawley, C. Phelan, and S. Nic Chormaic: N. J. Phys. **17** (2015) 013026.
25) W. Eickhoff and O. Krumpholz: Electronics Lett. **12** (1976) 405.
26) F. K. Fatemi and G. Beadie: Opt. Express **23** (2015) 3831.
27) J. E. Hoffman, F. K. Fatemi, G. Beadie, S. L. Rolston, and L. A. Orozco: Optica **2** (2015) 416.
28) F. K. Fatemi, J. E. Hoffman, P. Solano, E. F. Fenton, G. Beadie, S. L. Rolston, and L. A. Orozco: Optica **4** (2017) 157.
29) J. Carpenter, B. J. Eggleton, and J. Schröder: Opt. Lett. **41** (2016) 5580.
30) F. Le Kien and A. Rauschenbeutel: Phys. Rev. A **88** (2013) 063845.
31) A. Maimaiti, V. G. Truong, M. Sergides, I. Gusachenko, and S. Nic Chormaic: Sci. Rep. **5** (2015) 9077.
32) C. Phelan, T. Hennessy, and T. Busch: Opt. Express **21** (2013) 27093.
33) F. Le Kien, V. I. Balykin, and K. Hakuta: Phys. Rev. A **70** (2004) 063403.
34) J. Fu, X. Yin, N. Li, and L. Tong: Chinese Opt. Lett. **6** (2008) 112.
35) G. Brambilla, G. S. Murugan, J. S. Wilkinson, and D. J. Richardson: Opt. Lett. **32** (2007) 3041.
36) L. Xu, Y. Li, and B. Li: N. J. Phys. **14** (2012) 033020.
37) H. Lei, C. Xu, Y. Zhang, and B. Li: Nanoscale **4** (2012) 6707.
38) M. C. Frawley, I. Gusachenko, V. G. Truong, M. Sergides, and S. Nic Chormaic: Opt. Express **22** (2014) 16322.
39) A. Maimaiti, D. Holzmann, V. G. Truong, H. Ritsch, and S. Nic Chormaic: Sci. Rep. **6** (2016) 30131.
40) C. Sayrin, C. Clausen, B. Albrecht, P. Schneeweiss, and A. Rauschenbeutel: Optica **2** (2015) 353.

Laser word

Evanescent field

A propagating electromagnetic wave travelling through a homogeneous medium can be reflected or refracted when encountering an interface of another material with a lower refractive index. If the angle of incidence with respect to the normal of the interface is below the critical angle, the incident wave is partially reflected back and partially transmitted into the refracting media. However, if the angle of incidence is above the critical angle, total internal reflection, such as that of light propagating through an optical fiber, occurs. The transmitted wave is transformed into an evanescent wave along, and parallel to, the interface. Such waves are spatially confined at the interface with an exponentially decaying amplitude as the distance from the interface increases but with zero net energy flow. (Cindy Liza ESPORLAS)